AIAA JOURNAL
Vol. 56, No. 3, March 2018

Data Sampling Schemes for Microstructure Design with Vibrational Tuning Constraints

Arindam Paul*
Northwestern University, Evanston, Illinois 60208
Pinar Acar†
Virginia Tech, Blacksburg, Virginia 24061
Ruoqian Liu,* Wei-Keng Liao,‡ and Alok Choudhary§
Northwestern University, Evanston, Illinois 60208
Veera Sundararaghavan¶
University of Michigan, Ann Arbor, Michigan 48109
and
Ankit Agrawal**
Northwestern University, Evanston, Illinois 60208

DOI: 10.2514/1.J056170

Microstructures significantly impact the performance of sensitively engineered components, such as wireless impact detectors used in military vehicles or sensors used in aircrafts. These components can operate safely only within a certain range of frequencies, and frequencies outside that range can lead to instability because of resonance. This paper addresses optimization of the microstructure design to maximize the yield stress of a galfenol beam under vibration tuning constraints defined for the first torsional and bending natural frequencies by using a data-driven solution scheme. In this study, two carefully designed algorithms are used to sample the entire microstructure space. Classical optimization techniques often lead to a unique microstructural solution rather than yielding the complete space of optimal microstructures. Multiple optimal solutions are imperative for the practicality of design because conventional low-cost manufacturing processes can generate only a limited set of microstructures. The current data sampling-based methodology outperforms or is on par with other optimization techniques but also provides numerous near-optimal solutions, which is two to three orders of magnitude more than previous methods. Consequently, the proposed framework delivers a spectrum of optimal solutions in the microstructure space that can accelerate material development and reduce manufacturing costs.

Nomenclature

A	=	orientation distribution function
C	=	spatial correlation matrix
C_{eff}	=	effective stiffness vector
E_1	=	Young's modulus along axis 1, GPa
G_{12}	=	shear modulus in 1–2 plane, GPa
I_1	=	moment of inertia along axis 1
J	=	torsion constant
L	=	beam length
m	=	mass of the beam
q	=	volume normalization vector
r	=	orientation
S	=	compliance, 1/GPa
t	=	time
V	=	null space vector
Z	=	integers
α	=	constant
ε	=	volume-averaged strain
ϵ	=	very small value
σ	=	volume-averaged stress, MPa
χ	=	orientation-dependent property
ω_{1b}	=	first bending natural frequency, Hz
ω_{1t}	=	first torsional natural frequency, Hz

Received 21 March 2017; revision received 7 September 2017; accepted for publication 7 December 2017; published online 15 February 2018.

*Graduate Research Assistant, Department of Electrical Engineering and Computer Science.
†Assistant Professor, Department of Mechanical Engineering, Member AIAA.
‡Research Professor, Department of Electrical Engineering and Computer Science.
§Professor, Department of Electrical Engineering and Computer Science.
¶Associate Professor, Department of Aerospace Engineering. Member AIAA.
**Research Associate Professor, Department of Electrical Engineering and Computer Science.

I. Introduction

ONE of the primary aims of materials science and engineering research is to understand the association between materials' processing, structure, properties, and performance [1–10]. It is recognized that, even for a particular alloy system, variability in microstructure leads to a wide range of materials properties; and it substantially impacts the materials' performance, especially under extreme conditions. Thus, optimization of the microstructure can significantly improve the materials' performance. It is even more pertinent for sensitively engineered components that use magnetostrictive materials. Magnetostrictive materials undergo a change in shape or dimensions in response to a magnetic field. Furthermore, such materials can respond to external stresses by altering their magnetic states. The state of the art of magnetostrictive materials and their applications in a large variety of engineering applications was discussed by Olabi and Grunwald [11]. The authors also showed improvement in material features with the use of magnetostrictive materials. The magnetostrictive properties of different materials such as cubic Laves phases [such as Terbium-Iron alloy (TbFe2), Terbium-Iron-Dysprosium alloy (Terfenol D), and Samarium-Iron alloy (SmFe2)], as well as Fe-X alloys based on Fe-Ga and Fe-Al, were presented by Grossinger et al. [12]. The design of magnetostrictive actuators and transducers has been discussed in the literature [11,13–15]; however, the design of microstructural properties of magnetostrictive materials has not been studied

extensively yet. Galfenol is one such example of a magnetostrictive material [16,17]. It has been widely used in aerospace applications as a sensor material in beam-shaped structures. Galfenol can be processed using conventional rolling and wire drawing equipment; it can be machined using conventional mills and lathes, as well as welded to a wide array of materials. The potential of galfenol to develop desired anisotropic properties and flexibility regarding processing makes it a lucrative material. The single crystals of the galfenol material can provide large magnetostriction; however, their preparation is expensive. It is possible to develop comparable polycrystalline textured galfenol material as expensive single crystals by applying thermomechanical processes such as rolling and extrusion [18–20]. However, the control and prediction of the large changes in properties such as magnetostriction and yield strength during thermomechanical processing can be difficult. For instance, warm-rolled and annealed specimens retain high magnetostriction but are quite brittle, whereas cold-rolled specimens have high yield strength but lose their magnetostriction [21,22]. Experimental studies suggest that internal inhomogeneous strains introduced by microstructural changes play a major role in determining the final magnetostriction in galfenol [23]. The computation of a magnetostrictive strain of a polycrystalline galfenol material was studied before by Kumar and Sundararaghavan [17].

The orientation distribution function (ODF) is used to represent the microstructure. The ODF represents the volume fractions of the crystals of different orientations in the microstructure. The complete range of properties obtainable from the space of ODFs is represented using property closures, which are approximated by the space defined with the either upper or lower bound of a given property [16]. Upper-bound closure of stiffness values represents the range of properties obtainable by the upper-bound homogenization relation, whereas a lower-bound closure of compliance values shows the properties obtainable by the lower-bound homogenization equation. An approach that is gaining popularity in new materials development is selective optimization of certain properties of a material in a particular direction or plane while sacrificing the properties across other directions or planes that are not as important for the design problem [24].

There have been few efforts to optimize the microstructure to satisfy a given set of desired properties. Liu et al. [25] achieved this by directly sampling the ODF space using a data mining methodology. Some researchers have adopted sampling within the property hull and used a Fourier basis for discretizing the ODF [26–28]. In [16,29], Acar and Sundararaghavan derived an upper-bound solution approach; they started with generating samples in the space of macroelements (Young's modulus and shear modulus parameters) and then identified multiple optimal solutions through a linear solver. Acar and Sundararaghavan in [24] formulated a linear programming (LP) solution-based method for constructing property closures (for the homogenization relations considered here) by establishing the smallest convex region enveloping single crystal property points.

However, all these approaches used for constrained microstructure optimization lead to only one or, in some cases, a handful of solutions. Furthermore, the process for obtaining multiple solutions is often a trial-and-error-based method. On the other hand, conventional and economical manufacturing processes, such as metal forming and heat treatment, can generate only a limited set of microstructures [21,23,30]. Moreover, it may not be economically feasible to manufacture a single design solution [3]. Thus, there is a big incentive for developing approaches that can conceive a spectrum of optimal structures.

The paper proposes a data sampling-based scheme to find numerous near-optimal microstructures to maximize yield stress given vibrational design constraints. The proposed framework involves developing and executing sampling algorithms to generate possible ODF solutions satisfying the process limitations. The sampling algorithms developed in this work, partition and allocation schemes, are complementary to one another and ensure sampling of the entire feature space. Data points satisfying both the bending and torsional frequency constraints are generated. The proposed data sampling methodology outperforms (or is on par with) other optimization techniques and provides two to three orders of magnitude more of near-optimal solutions. Furthermore, our approach opens up additional opportunities for reducing the dimensionality of microstructure space to accelerate the process of achieving solutions that satisfy all the constraints by isolating ODF dimensions that are nonzero across a majority of near-optimal ODF solutions. The solution methodology presents an extensive approach; thusm it can be applied to different ODF representations such as finite element discretization and Fourier series expansion.

The rest of the paper is organized as follows. Section II provides a brief background of the microstructure, orientation distribution function, and galfenol alloy. Section III discusses some related works on the optimization of microstructure design for polycrystalline metals. Section IV describes the vibration tuning problem, and Sec. V presents the proposed data sampling-based methodology for optimization. In Sec. VI, the results are discussed and examined; finally, Sec. VII presents the conclusion and offers some recommendations for future studies.

II. Background

A. Property Representation in Rodrigues Space

The alloy microstructure consists of multiple crystals where each crystal has its distinct orientation. The ODF represents the volume fractions of the crystals of different orientations in the microstructure. The microstructure of the galfenol alloy system in this work is modeled using ODFs [31–34], which are represented by axis-angle parameterization of the orientation space [35]. Angle-axis representations elucidate an alternate way of representing orientations compared to Euler angles. The Rodrigues' parameterization is created by scaling the axis of rotation n as $r = n\tan(\theta/2)$, where θ is the rotation angle.

The ODF, which is a primary concept in texture analysis and anisotropy, is defined, based on a parameterization of the crystal lattice rotation. Orientation distributions can be described mathematically in any space appropriate to a continuous description of rotations [31,32,35]. The orientation space can be reduced to a subset called the fundamental region as a consequence of crystal symmetries. Each crystal orientation is depicted uniquely inside the fundamental region by a parameterization coordinate for the rotation r. The ODF, represented by $A(r)$, is the volume density of crystals of orientation r. The fundamental region is discretized into N independent nodes with N_{elem} finite elements and N_{int} integration points per element. A detailed explanation of the ODF discretization and volume-averaged equations has been provided in [16,24,25,29]. A single particular orientation or texture component is represented by each point in the orientation distribution. The orientation distribution information can be used to determine the presence of components and volume fractions, and it can predict the anisotropic properties of polycrystals. Although the term distribution function is used for ODFs, this is distinct from the "distribution function" used for the cumulative frequency curve in statistics. The ODF is a probability density but is constrained such that it is normalized to unity over the fundamental region. Figure 1 represents the finite element discretization of the orientation space of body centered cubic (BCC) galfenol.

The microstructure of an alloy comprises multiple crystals, and each crystal has an orientation. The generalized Hooke's law for the agglomeration is expressed as follows:

$$\langle \sigma_{ij} \rangle = C^{\text{eff}}_{ijkl} \langle \varepsilon_{kl} \rangle \tag{1}$$

where ε_{kl} and σ_{ij} represent the volume-averaged strain and yield stress of the agglomeration. C^{eff}_{ijkl} represents the tensor for effective stiffness in the given coordinate system. C^{eff} is the average over the aggregate of the crystals [24,36], where $\langle C \rangle$ represents the stiffness tensor for each crystal:

$$C^{\text{eff}} = \langle C \rangle \tag{2}$$

The averaging is performed over an aggregate of the crystal in a macroscale elementary volume. The crystal size and shape are ignored, and homogeneous deformity is assumed. The ODF

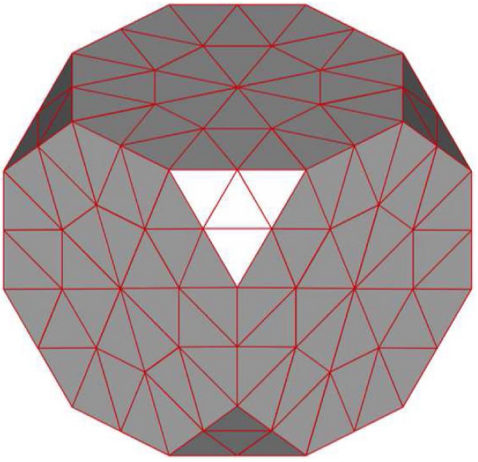

Fig. 1 Finite element discretization of the orientation space of BCC galfenol.

represents the volume density of each orientation in the microstructure. $\chi(r)$ represents the orientation-dependent property for single crystals, and $\langle\chi\rangle$ depicts the expected value:

$$\langle\chi\rangle = \int_R \chi(r)A(r,t)\,\mathrm{d}v \tag{3}$$

Using this parametrization, any polycrystal property can be expressed in a linear form as follows, where $A(r_m)$ is the value of the ODF at the mth integration point with the global coordinate r_m of the n^{th} element, $|J_n|$ is the Jacobian determinant of the nth element, w_m is the integration weight associated with the mth integration point, and $1/(1 + r_m \cdot r_m)^2$ represents the metric of the Rodrigues parameterization:

$$\begin{aligned}\langle\chi\rangle &= \chi(r)A(r,t)\,\mathrm{d}v \\ &= \sum_{n=1}^{N_{\text{elem}}}\sum_{m=1}^{N_{\text{int}}}\int_R \chi(r_m)A(r_m)w_m|J_n|\frac{1}{(1+r_m\cdot r_m)^2}\end{aligned} \tag{4}$$

A (which symbolizes the ODF) is a function of orientation r and time t during processing that satisfies the following normalization constraint:

$$\int_R A(r,t)\,\mathrm{d}v = 1 \tag{5}$$

The complete range of properties obtainable from the space of ODFs is represented using property closures, which are approximated by the space between the upper and lower bounds of the given property [16]:

$$\langle C\rangle = \int_R CA\,\mathrm{d}v \tag{6}$$

The upper-bound homogenization relation [in Eq. (6)] is based on the assumption of a constant strain throughout the thickness of the beam and is represented by the upper-bound closure of stiffness values. The upper-bound average or the Voigt average [37] is calculated by averaging the particular property (in this case, stiffness) by multiplying the ODF vector with the property vector. However, the lower-bound approach [in Eq. (7)] is based on the assumption of constant stress throughout the plate thickness. For the lower-bound average or the Reuss average [37], the inverse of the given property is averaged. For instance, in the following equation, compliance (C^{-1} or S), which is the inverse of stiffness, is averaged by using the lower-bound approach; and the equation is written for the compliance matrix. $\langle C\rangle$ and $\langle C^{-1}\rangle$ represent the volume-averaged macroscopic stiffness formulation in C and C^{-1} space. C^{-1} refers to compliance:

$$\langle C^{-1}\rangle = \int_R C^{-1}A\,\mathrm{d}v \tag{7}$$

The yield stress is computed for the upper- and lower-bound approaches in terms of single crystal yield strengths along the beam axis as follows:

$$\langle\sigma_y\rangle = \int \sigma_y A\,\mathrm{d}v \tag{8}$$

$$\langle\sigma_y^{-1}\rangle = \int \sigma_y^{-1}A\,\mathrm{d}v \tag{9}$$

B. Galfenol

Galfenol is a general name for an iron–gallium alloy, and the name was first associated in 1998 when it was discovered that adding gallium to iron increased its magnetostrictive effect [38,39]. A magnetostrictive material is used to harvest vibrational energy because of its property to change shape in response to a magnetic field. Galfenol also responds to external stresses by altering its magnetic state [40]. Researchers have found galfenol to demonstrate magnetostrictive strains of up to 400 ppm in single crystal form (which is more than 10 times that of α Fe [25]). Moreover, processing galfenol does not need any customized equipment. It can be processed using conventional rolling and wire drawing equipment, and it can be machined using standard mills and lathes; it can also be welded to a variety of materials [41]. Galfenol converts applied mechanical energy with high efficiency (around 70%) into magnetic energy, and vice versa [42]. Researchers have found that groups of contorted cells respond to a magnetic field by rotating their magnetic moments to align with the field that in turn, changes the exterior dimensions of the crystal. This contortion from the α Fe structure is responsible for galfenol's superior performance [43]. Adding gallium generates imperfections in iron's otherwise orderly lattice, thus improving the magnetostrictive property of the resultant alloy [44]. Single crystals of galfenol impart large magnetostriction, but the preparation of monocrystal galfenol is expensive. Hence, there is an impetus for the development of polycrystalline galfenol with favorable properties for various design problems [21,23,30]. Figure 2a represents the polycrystalline microstructure of galfenol, with different colors representing different crystal orientations. For this BCC structure, the Rodrigues fundamental region includes 76 independent nodal points (ODF values), as shown in Fig. 2b. It is noted that the red nodes in Fig. 2b are indicating the 76 independent ODF values, and the ODF values of the blue nodes can be computed using the crystallographic symmetries.

Among potential applications, galfenol has a wide application area in aerospace because it is usually used as a sensor material in beam-shaped structures. Moreover, electromagnetic waves travel three orders of magnitude faster than mechanical waves [42], with the impact information transmitted ahead of the waves created by the impact; and researchers have found that different configurations of galfenol energy harvesters can provide power to operate remote sensors and radios [45]. The presence of high stiffness [46], magnetostrictive strains [47,48], and yield strength [49] together makes galfenol ideal for many applications. Galfenol is used as actuators [50] in cantilever beam devices to generate sonar waves, or as sensors for measuring vibrations, or as energy-harvesting devices to produce electricity [25].

III. Related Works

Liu et al. [25,51] used a combination of random sampling and feature selection for the purpose of optimization of multiple design objectives, using a guided and generalized pattern search. Pattern search [52–55] finds a sequence of points $(x_0, x_1, x_2, \ldots)$ called a mesh, which approaches an optimal point by computing a sequence of points. The mesh is constructed by adding a starting point to a scalar multiple of a set of vectors. Once the pattern search algorithm identifies a point in the mesh that enhances the objective function at

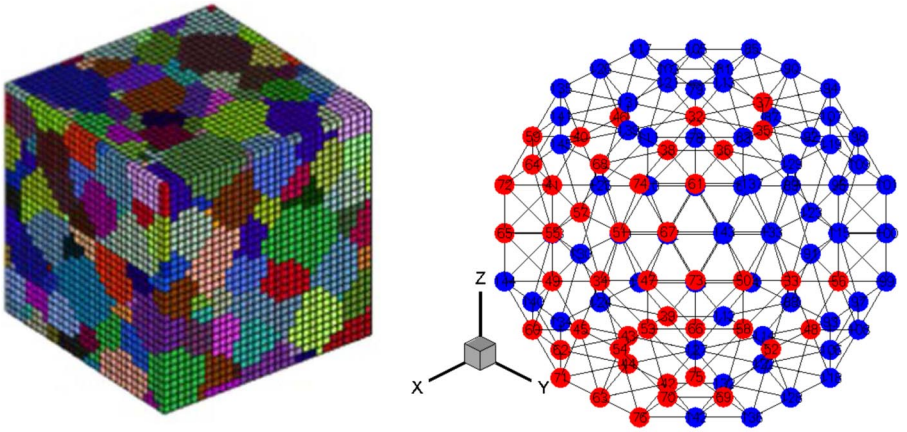

a) BCC galfenol microstructure

b) ODF representation, indicating the location of 76 independent nodes in the orientation space in red

Fig. 2 Finite element discretization of the orientation space of BCC galfenol.

the new point, this point becomes the new optimal point for the next step of the algorithm. The current problem is more convoluted as compared to Liu et al.'s [25,51] due to additional constraints on the first natural frequencies. These constraints make the problem much more complex and difficult to optimize using feature selection-based methods. It is because the neighborhood of a valid solution is often rendered invalid due to not meeting the constraints.

The optimization of the microstructure design of the galfenol vibration tuning problem with constraints has been studied earlier in [16,24,29]. In [16,29], the optimization problem was defined to maximize the yield stress of a cantilever beam under vibration tuning constraints. The authors derived an upper-bound solution approach, starting with generating samples in the space of macroelements (Young's modulus and shear modulus parameters), and then identified the multiple optimal solutions through a genetic algorithm-based solver. The linear solver scheme used a sampling technique called the incremental space filler (ISF) [56]. The ODFs for every global value were computed using the ISF; subsequently, the highest value of the yield stress among the feasible solutions was searched. Acar and Sundararaghavan in [24] formulated a linear programming [57] solution approach method for constructing property closures (for the homogenization relations considered here) by establishing the smallest convex region enveloping single crystal property points. LP is a rigorous and intuitive approach for the construction of property closures because closures are obtained as a result of property maximization or minimization. Connecting faces on the closure may contain polycrystals explicitly identified by the LP approach, which is well suited for other problems, such as identification of textures with desired property combinations where several properties are optimized simultaneously. The authors augmented the initial solution with null space to attain multiple solutions. However, the LP approach has few limitations. First, a LP method can be implemented only when the original nonlinear problem can be adapted to a linear problem. In addition, unlike the data sampling-based schemes proposed in this work, there is a limited number of multiple solutions possible. Furthermore, the procedure to obtain the multiplier to the null space is determined by trial and error. The advantage of a data sampling-based methodology is that it can explore the neighborhood of the optimal solution and generate many near-optimal solutions.

IV. Problem Description

We aim to explore the microstructure design constraint of a cantilevered galfenol beam for a vibration tuning problem with yielding objective. The vibration tuning puts a restriction on the ODF solutions to have a finite number of directions in the solution space. The number of independent ODF values is 76 at this time because galfenol has a BCC structure [25]. The design objective is determined as the maximization of yield stress, whereas the first bending and torsional frequencies are constrained for vibration tuning. The primary goal of the problem is to find the best microstructure design that maximizes the yield stress of the beam and satisfies the given vibration constraints.

The rationale behind constraining the operating frequencies is to eliminate possible dynamic instabilities: for instance, in sensor materials in aircraft beams [58,59]. The main goal of the problem is to find the best microstructure design that maximizes the yield stress of the beam and satisfies the given vibration constraints.

The torsional and bending frequency constraints are given by the following equations:

$$\omega_{1t} = \sqrt{\frac{G_{12}J}{\rho I_p}} \tag{10a}$$

$$\omega_{1b} = (\alpha L)^2 \sqrt{\frac{E_1 I_1}{mL^4}} \tag{10b}$$

where

$$\alpha L = 1.87510 \tag{11}$$

Here, $G_{12} = 1/S_{66}$, $E_1 = 1/S_{11}$, and S are the compliance elements ($S = C^{-1}$), E_1 is the Young's modulus along axis 1, and G_{12} is the shear modulus in the 1–2 plane. In these formulations, J is the torsion constant, ρ is density, I_p is the polar inertia moment, m is the unit mass, L is the length of the beam, and I_1 is the moment of inertia along axis 1. The mathematical formulation of the optimization problem is given as follows:

$$\max\ \sigma_y \tag{12}$$

$$A \geq 0 \tag{13}$$

$$\int A\,\mathrm{d}v = 1 \tag{14}$$

The optimization problem includes the unit volume constraint by definition [Eq. (14)]. The other constraints are the first natural frequencies to tune the beam vibration. In this problem, the length of the beam is taken as $L = 0.45$ m, and the beam is considered to have a rectangular cross section with dimensions of $a = 20$ mm and $b = 3$ mm. The values of the stiffness parameters for galfenol single crystals are taken as $C_{11} = 213$ GPa; $C_{12} = 174$ GPa, and $C_{44} = 120$ GPa [16,24,29]. C_{11}, C_{12}, C_{13}, and C_{14} comprise the most dominant elements in the stiffness matrix, which is a measure of the durability of a given material. The stiffness values of the polycrystal

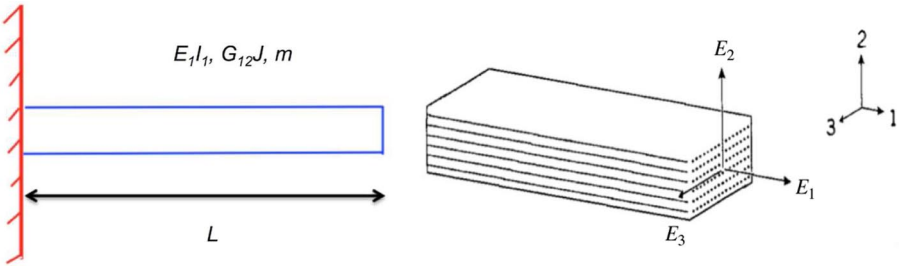

Fig. 3 Geometric representation of galfenol beam vibration problem.

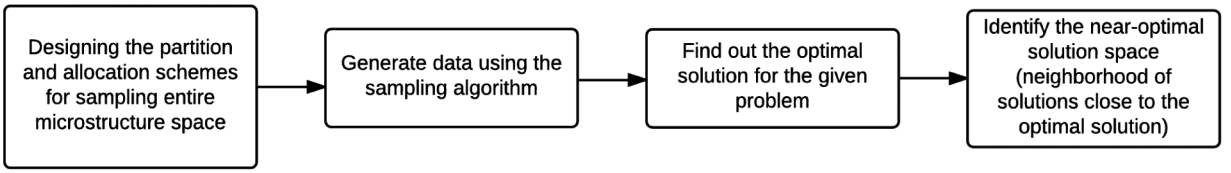

Fig. 4 Flow diagram of the proposed methodology. Upper- and lower-bound approaches for both sets of constraints are repeated for both problems.

are computed using the upper-bound averaging (C-space), whereas the lower-bound (C^{-1}-space) computation provides the compliance parameters. Figure 3 depicts the geometric representation of galfenol beam vibration problem. There are two sets of constraints presented in the following. Each set of constraints has a lower bound and an upper bound on the torsional and bending frequencies:

First set of constraints:

$$\text{subject to } 19.5 \text{ Hz} \leq \omega_{1t} \leq 21.5 \text{ Hz} \tag{15a}$$

$$\text{subject to } 120 \text{ Hz} \leq \omega_{1b} \leq 122.5 \text{ Hz} \tag{15b}$$

Second set of constraints:

$$\text{subject to } 21.5 \text{ Hz} \leq \omega_{1t} \leq 23.5 \text{ Hz} \tag{16a}$$

$$\text{subject to } 100 \text{ Hz} \leq \omega_{1b} \leq 114 \text{ Hz} \tag{16b}$$

It is important to note that both sets of constraints are specimens, and factual constraints may differ based on the real material design. Nonetheless, they are representative of a real-world design problem for magnetostrictive materials where there are bounds on the first natural frequencies.

V. Methodology

An overview of the proposed system is first presented, and then the algorithms proposed for sampling the ODF space for the given problem are explained.

A. Overview of the System

The paper proposes a two-step data-driven solution scheme to find optimal microstructure-satisfying performance requirements, as well as design and manufacturing constraints. The first phase of the approach involves developing and executing sampling algorithms to generate possible ODF solutions meeting the process limitations. The sampling algorithms (i.e., partition and allocation schemes) complement one another and ensure sampling of the entire feature space. Partition warrants that different permutations of nonzero ODF dimensions are explored for a given set of ODF dimensions. Allocation guarantees that all the ODF dimensions are explored sufficiently.

In the second step, data points are generated by satisfying both the bending and torsional frequency constraints. A future direction for reducing the dimensionality of microstructure space is highlighted that can accelerate the process of achieving solutions satisfying all the constraints by isolating ODF dimensions that are mostly nonzero across a majority of near-optimal ODF solutions. Figure 4 illustrates the steps in the proposed framework in a flow diagram.

B. Algorithms

Two sampling techniques, the partition and allocation algorithms, developed in the proposed work are presented. The algorithms address the problem of sufficiently sampling the problem space and generate ODFs fulfilling the constraints in the problem objective.

1. *Partition Method*

In this method, the unit length is divided into k small segments, and k is decided by a limit set as D. D is the number of dimensions and, in the case of galfenol, D is equal to 76. Note that $k-1$ random cuts between the interval [0,1] (Fig. 5) are made, where k is the number of nonzero ODF dimensions in the ODF vector. It is iterated from 1 to $D-1$ with an increasing number of samples generated with regard to k, and then it is downsampled to 1000 for each iteration; except when $k=1$, D samples exist (corresponding to D single crystals) and are all used. The steps of the partition algorithm (pseudocode) are outlined in Algorithm 1.

2. *Allocation Method*

In this method, k values are randomly generated at a time. It continues only when the sum S is less than the whole (in this case, one). As mentioned previously, the sum of the product of the volume fraction vf and density functions df across each dimension must add up to one. The threshold is updated to the remainder $1-S$ and continues until this remainder is sufficiently small. Note that $k=1$ is the trivial case where the product of vf and df equals to one. The steps of the allocation algorithm (pseudocode) are presented in Algorithm 2.

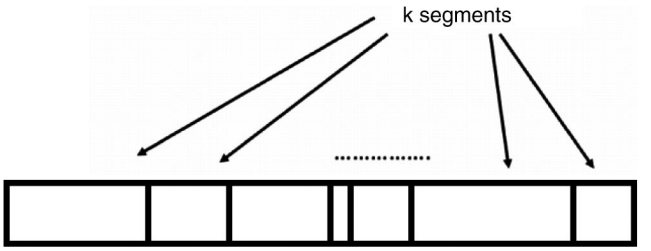

Fig. 5 Partition algorithm: The unit length is divided into k small segments.

Algorithm 1 Partition algorithm

```
procedure PARTITION
  D ∈ Z
  for k ∈ {1, ..., D − 1}, do
    for i ∈ {1, ..., 1000}, do
      for cut ∈ {1, ..., k − 1}, do
        Make an arbitrary cut
      end for                          ▷ Sample with k cuts generated
    end for                            ▷ 1000 samples with different cuts
  end for
  return
end procedure
```

Algorithm 2 Allocation algorithm

```
procedure ALLOCATION
  Generate a random k ∈ {1, ..., 76}
  Sum←0
  for i ∈ {1, ..., k}, do
    Sum←Sum + vf(i)*df(i)
    remainder←1 − Sum
    if remainder <ϵ, then             ▷ ϵ: very small value
      break
    else
      continue
    end if
  end for
  return
end procedure
```


Both the partition and allocation methods are based on the heuristic that, in a valid microstructure obeying all the constraints, only a few of all the dimensions of the ODF vector are nonzero. However, these two methods are complementary or reciprocal to each other and ensure that the entire feature space is sampled sufficiently. Although the allocation method attempts to find a minimal subset of ODF dimensions that would be nonzero, generating a polycrystal solution, the partition method seeks to widen the search across all 76 dimensions.

VI. Results

In this section, we evaluate the proposed data-driven approach in yielding optimal and near-optimal solutions, and we find that it outperforms or matches previous state-of-the-art methods and produces numerous near-optimal solutions, which is one of the most significant contributions of this study. Table 1 presents the total number of near-optimal solutions or, in other words, solutions that are proximal to the optimal solutions. The near-optimal solutions of this problem correspond to different designs having the same or similar values for yield stress. The algorithms were executed to produce around 5 million valid (which obey all the constraints) solutions. It took averages of 112.21 and 303.45 ms to generate a valid sample for the partition and the allocation scheme, respectively.

Optimization techniques including the methods used by Acar and Sundararaghavan such as a genetic algorithm [16] or linear programming-based [24] scheme, lead to a unique microstructural solution, or sometimes a few microstructural solutions. Acar and Sundararaghavan found multiple solutions by augmenting the original solution with null space [24]. Acar and Sundararaghavan [24] previously studied an LP approach to identify the optimal processing routes, which can produce the optimum microstructure designs of the same galfenol vibration tuning problem. One of the limitations of their approach for vetting equivalent solutions was that it only searched for identical optimal values. However, for practical design applications, a near-optimal solution is adequate as long as the constraints are strictly obeyed and the near-optimal solutions are proximal to the optimal solution. For all four problems (upper- and lower-bound approaches for two sets of constraints), three to nine near-optimal solutions with a neighborhood of 10^{-4} (from the optimal solution) are discovered. Furthermore, between 89 and 402 solutions in a neighborhood of 10^{-3} and between 147 and 1579 solutions in a neighborhood of $5 * 10^{-3}$, across all the categories, are identified. As described before, obtaining multiple optimal solutions is critical because traditional low-cost manufacturing processes can only generate a limited set of microstructures. Although a single solution may not be economically feasible to manufacture, hundreds or thousands of near-optimal solutions can accelerate the speed of materials development. Therefore, it provides flexibility to produce solutions that are selectively cost effective and improve the overall efficiency of manufacturing immensely.

Liu et al.'s [25,51] approach of using guided and generalized pattern search methods was compared with the proposed data-driven methodology for the current design problem. However, neither of

Table 1 Number of solutions within 0.01, 0.1, and 0.5% of the optimal solutions[a]

Constraint	Bound	Within 0.01%	Within 0.1%	Within 0.5%
1	Upper	3	89	147
1	Lower	9	92	222
2	Upper	7	402	2015
2	Lower	3	116	1579

[a]For each set of constraints [Eqs. (15a) and (16a)], 5 million valid data points were generated.

Table 2 Summary of the results: The yield stress σ_y, Young's modulus E_1, shear modulus G_{12}, and bending ω_{1b} and torsional ω_{1t} frequencies of the optimal solutions generated by the proposed method for both sets of constraints [Eqs. (15a) and (16a)]

Constraint	Bound	σ_y, MPa	E_1, GPa	G_{12}, GPa	ω_{1b}, Hz	ω_{1t}, Hz
1	Upper	385.237	209.546	77.313	120.006	21.341
1	Lower	385.113	235.905	82.316	121.272	21.344
2	Upper	388.089	153.160	93.723	102.649	23.497
2	Lower	387.134	184.679	92.772	112.661	23.377

Table 3 Comparison of the maximum yield stress achieved for the two sets of constraints with the proposed approach and the previous state-of-the art genetic algorithm (GA) solver [16] approach for microstructure design with process constraints (upper bound)[a]

Constraint	Bound	σ_y (current), MPa	σ_y (GA), MPa	ω_{1b} (current), Hz	ω_{1b} (GA), Hz	ω_{1t} (current), Hz	ω_{1t} (GA), Hz
1	Upper	385.237	384.126	120.006	120.210	21.341	21.498
2	Upper	388.089	308.446	102.589	113.918	23.482	23.485

[a]The yield stress σ_y and bending ω_{1b} and torsional ω_{1t} frequencies of the optimal solutions are generated by both methods.

Table 4 Comparison of the maximum yield stress achieved for the two sets of constraints with the proposed approach and the previous state-of-the-art LP [24] approach for the microstructure design with process constraints (lower bound)[a]

Constraint	Bound	σ_y (current), MPa	σ_y (LP), MPa	ω_{1b} (current), Hz	ω_{1b} (LP), Hz	ω_{1t} (current), Hz	ω_{1t} (LP), Hz
1	Lower	385.113	385.650	121.272	120.020	21.344	21.500
2	Lower	387.134	387.259	106.519	100.000	23.477	23.499

[a]The yield stresses σ_y and bending ω_{1b} and torsional ω_{1t} frequencies of the optimal solutions are generated by both methods.

these approaches converged to an optimal solution for the current problem. Although both problems had a yielding objective for a cantilevered galfenol beam, the current problem is more convoluted as compared to Liu et al.'s because of additional constraints on the first natural frequencies. Pattern search finds a sequence of points to approach an optimal point. Due to the added constraints in the current problem, pattern search algorithms fail to converge to an optimal solution [60]. For pattern search to successfully reach an optimal solution, it requires a series of valid points at each iteration of the optimization process.

Table 2 illustrates the optimal yield stress values and Young's modulus, shear modulus, and bending and torsional frequencies obtained by the proposed method for both sets of constraints and bounds.

In their previous works [16,29], Acar and Sundararaghavan used a genetic algorithm-based scheme to solve the upper-bound approach. In a later work, Acar and Sundararaghavan [24] converted the upper-bound approach to a lower-bound approach that involved converting the problem from stiffness domain to compliance (reciprocal of stiffness) domain. Hence, by converting the original problem into a linear problem, Acar and Sundararaghavan arrived at an LP solution for the constrained microstructure design problem. The proposed data-driven approach is compared with the methods advanced by Acar and Sundararaghavan because their approach outperformed

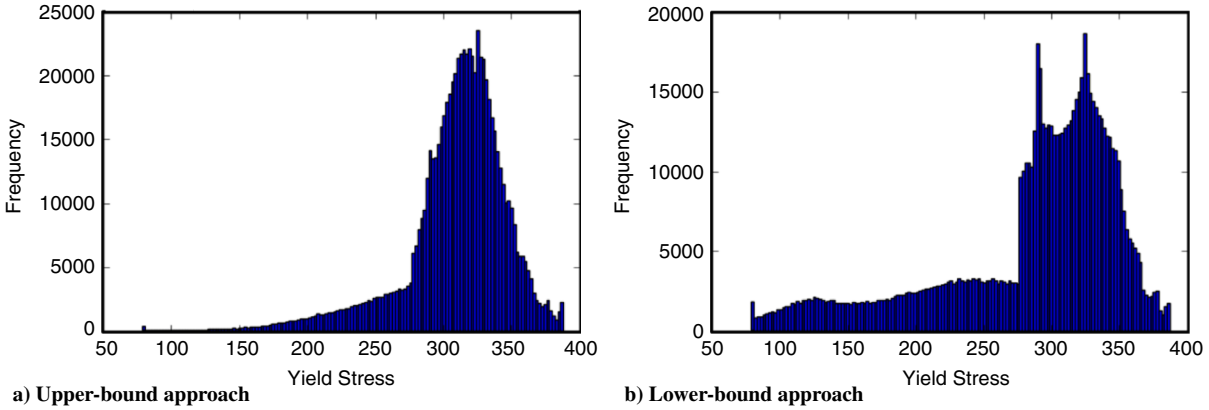

a) Upper-bound approach **b) Lower-bound approach**

Fig. 6 Frequency distribution of yield stress values for first set of constraints.

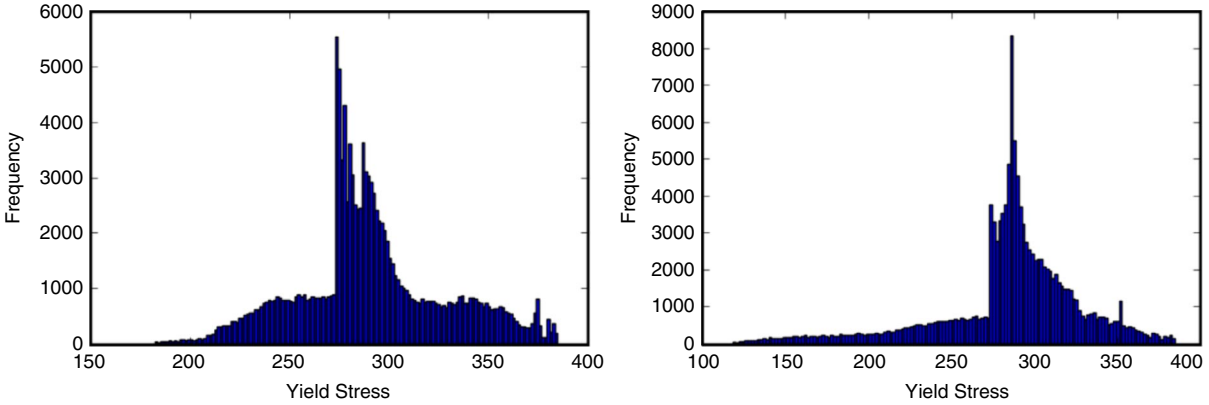

a) Upper-bound approach **b) Lower-bound approach**

Fig. 7 Frequency distribution of yield stress values for second set of constraints.

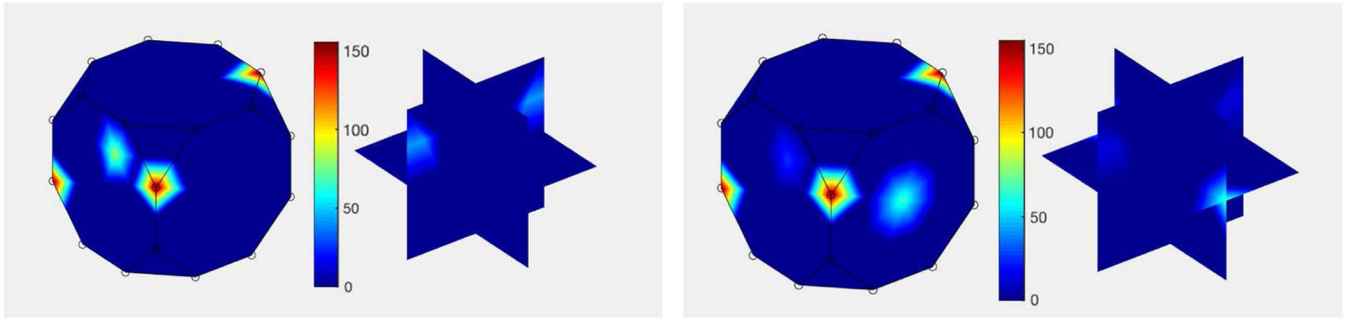

a) Upper-bound approach b) Lower-bound approach

Fig. 8 Finite element microstructure of optimal ODF examples for the first set of frequency constraints.

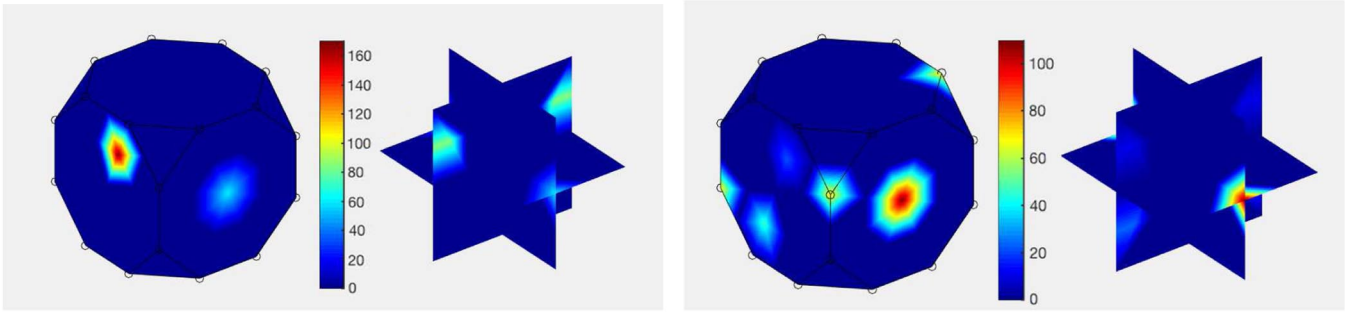

a) Upper-bound approach b) Lower-bound approach

Fig. 9 Finite element microstructure of optimal ODF examples for the second set of frequency constraints.

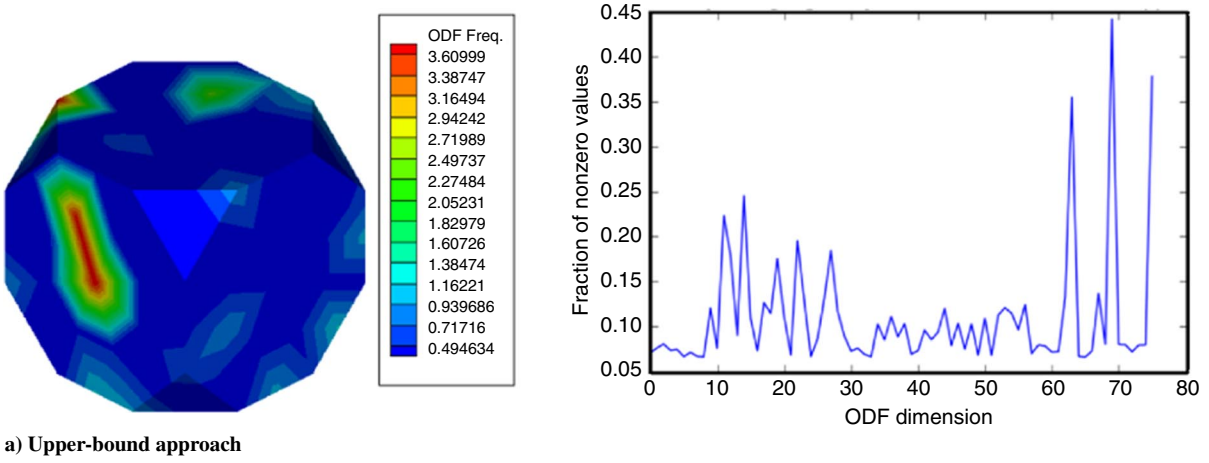

a) Upper-bound approach

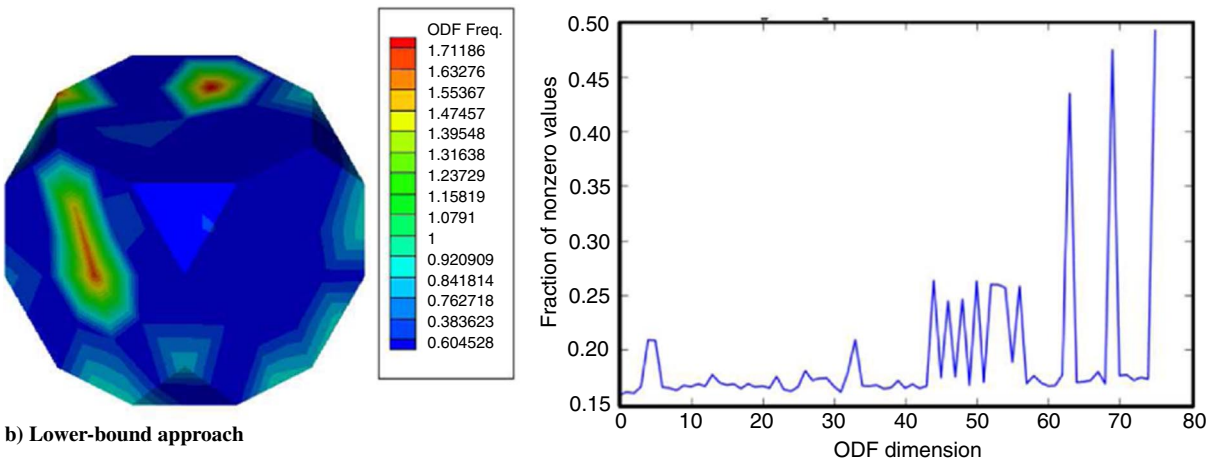

b) Lower-bound approach

Fig. 10 Finite element plots for highest 1% yield values for the first set of constraints.

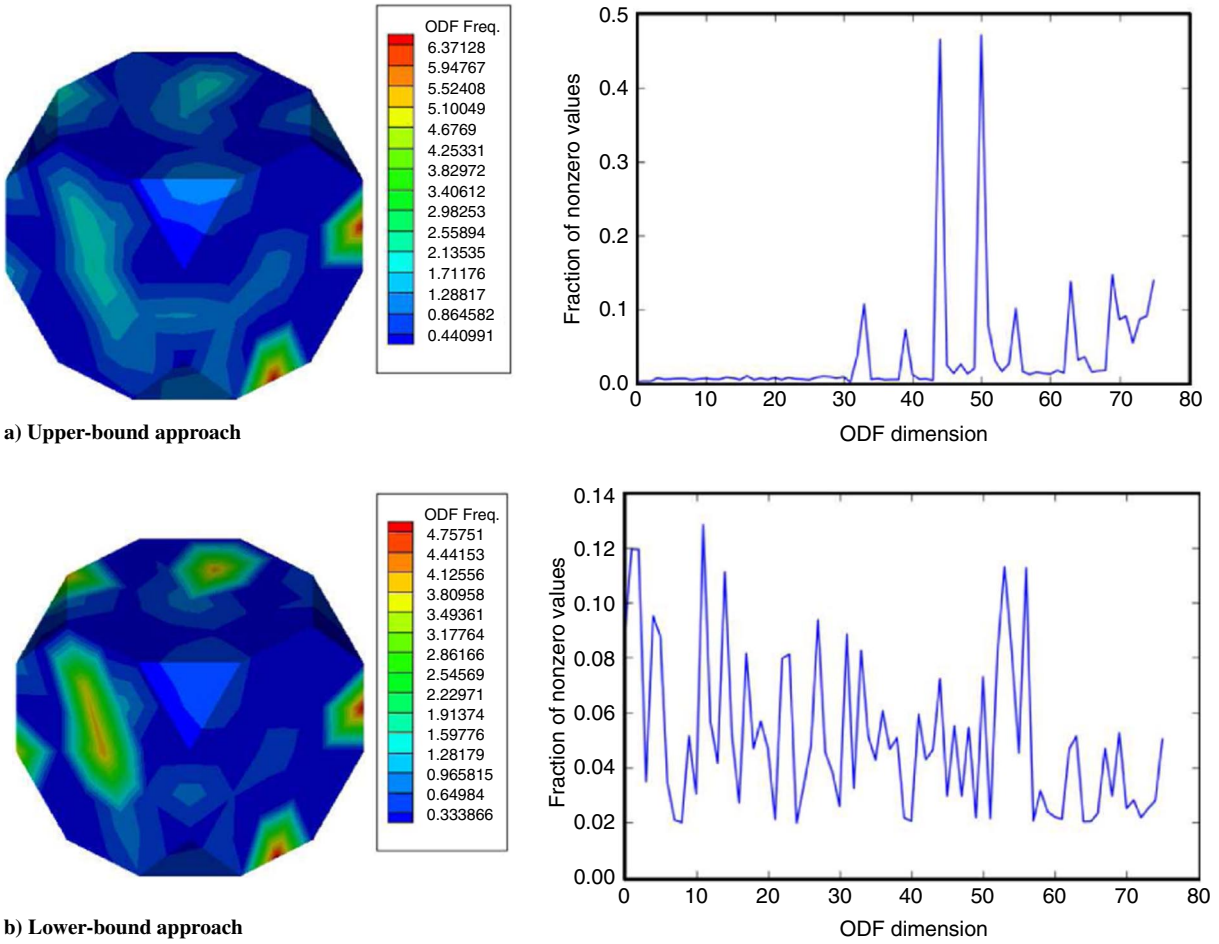

Fig. 11 Finite element plots for highest 1% yield values for the second set of constraints.

other optimization methods. For the upper- and lower-bound approaches, our solutions are compared against the genetic algorithm-based scheme and LP-based methods, respectively. The proposed data sampling approach based on the sampling algorithms surpasses the yield stresses obtained from the genetic algorithm-based solver for the upper-bound approach (as shown in Table 3). In particular, we get an improvement of more than 25% for the upper-bound approach on the first set of objectives against the previous state-of-the art approach. Additionally, the results for the lower bound are comparable to the optimal values achieved by the LP method (Table 4). It is important to note that only the LP solution (used for the lower-bound approach by Acar and Sundararaghavan [24]) yields the theoretical maximum value, which is in contrast to the genetic algorithm solver scheme used by them for the upper-bound approach [16].

Figures 6 and 7 represent the frequency distribution of yield stress values for upper and lower bounds for the first and second sets of constraints, respectively. Figures 8 and 9 depict the optimal upper- and lower-bound ODF solutions for the two constraints, respectively. Figures A1 and A2 in the appendix provide more examples of upper- and lower-bound ODF solutions.

A sensitivity analysis is performed by representing the distribution ODF and frequency plot (inset) of the top/highest 1% yield stress values across the 76 ODF dimensions (Figs. 10 and 11). The figures exhibit the fraction (or percentage) of nonzero ODFs in the ODF vectors that yield high-stress values, in the case of both upper- and lower-bound solutions for both sets of constraints. The peaks in the frequency plots represent the ODF dimensions that are nonzero across the majority of ODF vectors, yielding the highest objective value (in this case, yield stress). The distribution ODFs in these figures do not exhibit the actual values. Rather, they represent the percentage of occurrence of the ODF dimensions in the top 1% of the solutions. It is observed that the sensitivity of the near-optimum solutions to the ODFs for the lower- and upper-bound approaches are similar, especially for the first set of constraints. Although the computation of intermediate properties in the case of upper- or lower-bound solutions is different (stiffness and compliance, respectively), this is admissible because the same objective function is being solved. The figures signify that a small number of ODF dimensions can predominantly influence the solution space proximal to the optimal value. This can motivate the development of future sampling approaches for ODF vectors to iteratively adapt to sample across only a few ODF dimensions instead of all to accelerate the data-generation process.

One weakness of the proposed data-driven method is its higher time cost as compared to LP methods. However, traditional optimization techniques using combinatorial search methods or evolutionary algorithms are also time consuming. Our framework attempts to search the entire sample space to attain the optimal or near-optimal solutions. Besides, it should be emphasized that the proposed sampling algorithms are designed to work, even for the more difficult problem of nonlinear optimization. A heuristic search using data-driven approaches is beneficial for solving problems in which the objective function has a nonconvex relation to its set of constraints. Another major advantage of the proposed sampling scheme is achieving numerous optimal and near-optimal solutions that can, in turn, reduce the time and effort for the transition between design and processing.

VII. Conclusions

The selection of materials and geometries to maximize or minimize a given property has been a cardinal problem in materials science. The potential of data-driven approaches for solving a constrained microstructure design problem for both upper- and lower-bound methods is expounded by the proposed strategy. The current approach arrives at a higher (or, in few cases, equivalent)

optimal value than the previous state-of-the-art methods. The data-generation strategies attempt to explore the entire sample space and generate numerous near-optimal solutions (about 100–1000; i.e., two to three orders of magnitude more than prior methods). Previous approaches including LP techniques led to one or multiple optimal solutions. Numerous near-optimal solutions give the flexibility to use traditional low-cost manufacturing processes such as forming and heat treatment. These processes can generate only a limited set of microstructures; frequently, manufacturing from a single optimal solution may not be feasible.

Leveraging data-driven techniques can play an essential role in the expedition of a precise design of materials with process constraints. This study has demonstrated the power of carefully designed sampling approaches by identifying multiple near-optimal solutions for a nonlinear optimization problem, and it is expected to inspire the development of alternative sampling schemes, building upon the ones proposed in this work, that can reach optimal solutions faster and deliver numerous near-optimal solutions. Furthermore, with parallel computing technologies becoming inexpensive, especially graphical processing units computing, distributed implementations of the current algorithm can significantly diminish the optimization time. The proposed approach for maximizing the yield stress under process constraints using data sampling algorithms can be extended for property optimizations for other nonlinear design limitations and other materials. The sampling schemes are generalizable and independent of the problem domain, and they can be used in other scientific domains as well.

The analysis for the constrained microstructure optimization problem depicts that certain combinations of ODF dimensions are nonzero more often in the ODF vector of the near-optimal solutions. The proposed work provides a future direction for feedback-aware sampling that can iteratively incentivize distinct ODF dimensions that yield ODF vectors with higher objective values, which can be investigated to accelerate the process of attaining optimal or near-optimal solutions.

Appendix: More Optimal ODF Solutions

Acknowledgments

This work is supported primarily by the U.S. Air Force Office of Scientific Research's Multidisciplinary University Research Initiative award FA9550-12-1-0458. Partial support is also acknowledged from the following grants: National Institute of Standards and Technology award 70NANB14H012; National Science Foundation award CCF-1409601; U.S. Department of Energy awards DE-SC0007456 and DE-SC0014330; and the Northwestern Data Science Initiative.

References

[1] Olson, G. B., "Computational Design of Hierarchically Structured Materials," *Science*, Vol. 277, No. 5330, 1997, pp. 1237–1242. doi:10.1126/science.277.5330.1237

[2] Agrawal, A., and Choudhary, A., "Perspective: Materials Informatics and Big Data: Realization of the "Fourth Paradigm" of Science in Materials Science," *APL Materials*, Vol. 4, No. 5, 2016, Paper 053208. doi:10.1063/1.4946894

[3] Sundararaghavan, V., and Zabaras, N., "Linear Analysis of Texture–Property Relationships Using Process-Based Representations of Rodrigues Space," *Acta Materialia*, Vol. 55, No. 5, 2007, pp. 1573–1587. doi:10.1016/j.actamat.2006.10.019

[4] Agrawal, A., Deshpande, P. D., Cecen, A., Basavarsu, G. P., Choudhary, A. N., and Kalidindi, S. R., "Exploration of Data Science Techniques to Predict Fatigue Strength of Steel from Composition and Processing Parameters," *Integrating Materials and Manufacturing Innovation*, Vol. 3, No. 1, 2014, pp. 1–19. doi:10.1186/2193-9772-3-8

[5] Ward, L., Agrawal, A., Choudhary, A., and Wolverton, C., "A General-Purpose Machine Learning Framework for Predicting Properties of Inorganic Materials," *NPJ Computational Materials*, Vol. 2, No. 1, 2016, Paper 16028. doi:10.1038/npjcompumats.2016.28

[6] Liu, R., Yabansu, Y. C., Yang, Z., Choudhary, A. N., Kalidindi, S. R., and Agrawal, A., "Context Aware Machine Learning Approaches for Modeling Elastic Localization in Three-Dimensional Composite Microstructures," *Integrating Materials and Manufacturing Innovation*,

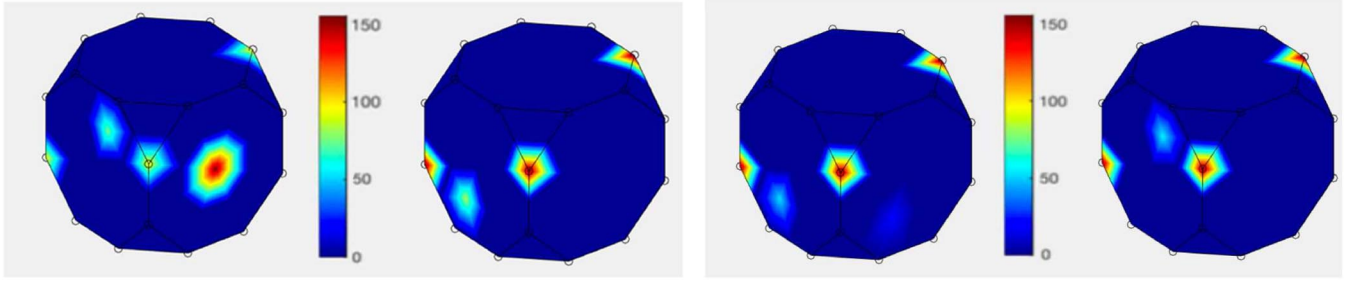

a) Upper-bound solution b) Lower-bound solution

Fig. A1 More finite element microstructure examples of near-optimal ODF solutions for the first set of constraints.

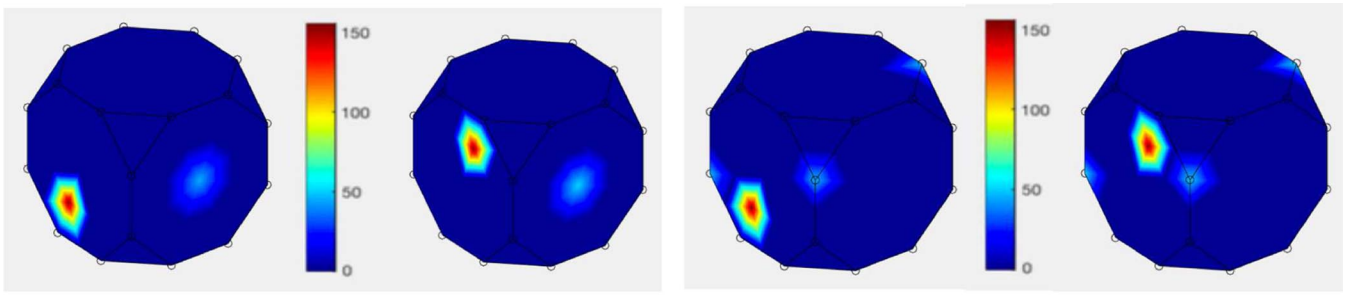

a) Upper-bound solution b) Lower-bound solution

Fig. A2 More finite element microstructure examples of near-optimal ODF solutions for the second set of constraints.

Vol. 1, 2017, pp. 1–0.
doi:10.1007/s40192-017-0094-3
[7] Deshpande, P., Gautham, B., Cecen, A., Kalidindi, S., Agrawal, A., and Choudhary, A., "Application of Statistical and Machine Learning Techniques for Correlating Properties to Composition and Manufacturing Processes of Steels," *Proceedings of the 2nd World Congress on Integrated Computational Materials Engineering (ICME)*, Springer, New York, 2013, pp. 155–160.
doi:10.1002/9781118767061.ch25
[8] Liu, R., Agrawal, A., Liao, W.-K., Choudhary, A., and De Graef, M., "Materials Discovery: Understanding Polycrystals from Large-Scale Electron Patterns," *2016 IEEE International Conference on Big Data (Big Data)*, IEEE Publ., Piscataway, NJ, 2016, pp. 2261–2269.
doi:10.1109/BigData.2016.7840857
[9] Meredig, B., Agrawal, A., Kirklin, S., Saal, J. E., Doak, J., Thompson, A., Zhang, K., Choudhary, A., and Wolverton, C., "Combinatorial Screening for New Materials in Unconstrained Composition Space with Machine Learning," *Physical Review B: Solid State*, Vol. 89, No. 9, 2014, Paper 094104.
doi:10.1103/PhysRevB.89.094104
[10] Liu, R., Yabansu, Y. C., Agrawal, A., Kalidindi, S. R., and Choudhary, A. N., "Machine Learning Approaches for Elastic Localization Linkages in High-Contrast Composite Materials," *Integrating Materials and Manufacturing Innovation*, Vol. 4, No. 1, 2015, p. 13.
doi:10.1186/s40192-015-0042-z
[11] Olabi, A.-G., and Grunwald, A., "Design and Application of Magnetostrictive Materials," *Materials and Design*, Vol. 29, No. 2, 2008, pp. 469–483.
doi:10.1016/j.matdes.2006.12.016
[12] Grossinger, R., Turtelli, R. S., and Mehmood, N., "Materials with High Magnetostriction," *IOP Conference Series: Materials Science and Engineering*, Vol. 60, IOP Publ., 2014, Paper 012002.
doi:10.1088/1757-899X/60/1/012002
[13] Claeyssen, F., Lhermet, N., Le Letty, R., and Bouchilloux, P., "Actuators, Transducers and Motors Based on Giant Magnetostrictive Materials," *Journal of Alloys and Compounds*, Vol. 258, Nos. 1–2, 1997, pp. 61–73.
doi:10.1016/S0925-8388(97)00070-4
[14] Zhang, H., Zhang, T., and Jiang, C., "Design of a Uniform Bias Magnetic Field for Giant Magnetostrictive Actuators Applying Triple-Ring Magnets," *Smart Materials and Structures*, Vol. 22, No. 11, 2013, Paper 115009.
doi:10.1088/0964-1726/22/11/115009
[15] Yamamoto, Y., Eda, H., and Shimizu, J., "Application of Giant Magnetostrictive Materials to Positioning Actuators," *Proceedings, of the 1999 IEEE/ASME International Conference on Advanced Intelligent Mechatronics*, IEEE Publ., Piscataway, NJ, 1999, pp. 215–220.
doi:10.1109/AIM.1999.803169
[16] Acar, P., and Sundararaghavan, V., "Utilization of a Linear Solver for Multiscale Design and Optimization of Microstructures in an Airframe Panel Buckling Problem," *57th AIAA/ASCE/AHS/ASC Structures, Structural Dynamics, and Materials Conference*, AIAA Paper 2016-0156, 2016.
doi:10.2514/6.2016-0156
[17] Kumar, A., and Sundararaghavan, V., "Simulation of Magnetostrictive Properties of Galfenol Under Thermomechanical Deformation," *Finite Elements in Analysis and Design*, Vol. 127, 2017, pp. 1–5.
doi:10.1016/j.finel.2016.11.009
[18] Kellogg, R., Russell, A., Lograsso, T., Flatau, A., Clark, A., and Wun-Fogle, M., "Tensile Properties of Magnetostrictive Iron–Gallium Alloys," *Acta Materialia*, Vol. 52, No. 17, 2004, pp. 5043–5050.
doi:10.1016/j.actamat.2004.07.007
[19] Restorff, J., Wun-Fogle, M., and Clark, A., "Measurement of d_{15} in Fe_{100-x} Ga_x ($x = 12.5$, 15, 18.4, 22), Fe_{50} Co_{50}, and Fe_{81} Al_{19} Highly Textured Polycrystalline Rods," *Journal of Applied Physics*, Vol. 103, No. 7, 2008, Paper 07B305.
doi:10.1063/1.2832667
[20] Mahadevan, A., Evans, P., and Dapino, M., "Dependence of Magnetic Susceptibility on Stress in Textured Polycrystalline $Fe_{81.6}$ $Ga_{18.4}$ and $Fe_{79.1}$ $Ga_{20.9}$ Galfenol Alloys," *Applied Physics Letters*, Vol. 96, No. 1, 2010, Paper 012502.
doi:10.1063/1.3280374
[21] Cheng, L. M., Nolting, A. E., Voyzelle, B., and Galvani, C., "Deformation Behavior of Polycrystalline Galfenol at Elevated Temperatures," *Proceedings of the SPIE: Behavior and Mechanics of Multifunctional and Composite Materials*, edited by M. J. Dapino, Vol. 6526, 2007, Paper 65262N.
doi:10.1117/12.720664
[22] Na, S.-M., and Flatau, A. B., "Deformation Behavior and Magnetostriction of Polycrystalline Fe–Ga–X (X = B, C, Mn, Mo, Nb, Nb C) Alloys," *Journal of Applied Physics*, Vol. 103, No. 7, 2008, Paper 07D304.
doi:10.1063/1.2838772
[23] Srisukhumbowornchai, N., and Guruswamy, S., "Crystallographic Textures in Rolled and Annealed Fe–Ga and Fe–Al Alloys," *Metallurgical and Materials Transactions A*, Vol. 35, No. 9, 2004, pp. 2963–2970.
doi:10.1007/s11661-004-0243-0
[24] Acar, P., and Sundararaghavan, V., "Linear Solution Scheme for Microstructure Design with Process Constraints," *AIAA Journal*, Vol. 54, No. 12, 2016, pp. 4022–4031.
doi:10.2514/1.J055247
[25] Liu, R., Kumar, A., Chen, Z., Agrawal, A., Sundararaghavan, V., and Choudhary, A., "A Predictive Machine Learning Approach for Microstructure Optimization and Materials Design," *Scientific Reports*, Vol. 5, 2015.
doi:10.1038/srep11551
[26] Adams, B. L., Henrie, A., Henrie, B., Lyon, M., Kalidindi, S., and Garmestani, H., "Microstructure-Sensitive Design of a Compliant Beam," *Journal of the Mechanics and Physics of Solids*, Vol. 49, No. 8, 2001, pp. 1639–1663.
doi:10.1016/S0022-5096(01)00016-3
[27] Kalidindi, S. R., Houskamp, J. R., Lyons, M., and Adams, B. L., "Microstructure Sensitive Design of an Orthotropic Plate Subjected to Tensile Load," *International Journal of Plasticity*, Vol. 20, No. 8, 2004, pp. 1561–1575.
doi:10.1016/j.ijplas.2003.11.007
[28] Fast, T., Knezevic, M., and Kalidindi, S. R., "Application of Microstructure Sensitive Design to Structural Components Produced From Hexagonal Polycrystalline Metals," *Computational Materials Science*, Vol. 43, No. 2, 2008, pp. 374–383.
doi:10.1016/j.commatsci.2007.12.002
[29] Acar, P., and Sundararaghavan, V., "Utilization of a Linear Solver for Multiscale Design and Optimization of Microstructures," *AIAA Journal*, Vol. 54, No. 5, 2016, pp. 1751–1759.
doi:10.2514/1.J054822
[30] Na, S.-M., and Flatau, A. B., "Secondary Recrystallization, Crystallographic Texture and Magnetostriction in Rolled Fe–Ga Based Alloys," *Journal of Applied Physics*, Vol. 101, No. 9, 2007, Paper 09N518.
doi:10.1063/1.2712822
[31] Bunge, H.-J., *Texture Analysis in Materials Science: Mathematical Methods*, Elsevier, New York, 2013, pp. 3–41.
[32] Heinz, A., and Neumann, P., "Representation of Orientation and Disorientation Data for Cubic, Hexagonal, Tetragonal and Orthorhombic Crystals," *Acta Crystallographica Section A: Foundations of Crystallography*, Vol. 47, No. 6, 1991, pp. 780–789.
doi:10.1107/S0108767391006864
[33] Kocks, U. F., Tomé, C. N., and Wenk, H.-R., *Texture and Anisotropy: Preferred Orientations in Polycrystals and their Effect on Materials Properties*, Cambridge Univ. Press, New York, 2000, pp. 44–77.
[34] Randle, V., and Engler, O., *Introduction to Texture Analysis: Macrotexture, Microtexture and Orientation Mapping*, CRC Press, Boca Raton, FL, 2000, pp. 128–132.
[35] Kumar, A., and Dawson, P., "Computational Modeling of fcc Deformation Textures over Rodrigues' Space," *Acta Materialia*, Vol. 48, No. 10, 2000, pp. 2719–2736.
doi:10.1016/S1359-6454(00)00044-6
[36] Taylor, G. I., "Analysis of Plastic Strain in a Cubic Crystal," *Stephen Timoshenko 60th Anniversary Volume*, 1938, pp. 218–224.
doi:10.1016/0022-5096(57)90058-3
[37] Chung, D., and Buessem, W., "The Elastic Anisotropy of Crystals," *Journal of Applied Physics*, Vol. 38, No. 5, 1967, pp. 2010–2012.
doi:10.1063/1.4962996
[38] Wang, H., Zhang, Y., Wu, R., Sun, L., Xu, D., and Zhang, Z., "Understanding Strong Magnetostriction in Fe100 xGax Alloys," *Scientific Reports*, Vol. 3, 2013.
doi:10.1038/srep03521
[39] Shi, R., Zhou, N., Niezgoda, S., and Wang, Y., "Microstructure and Transformation Texture Evolution During α Precipitation in Polycrystalline α/β Titanium Alloys—A Simulation Study," *Acta Materialia*, Vol. 94, 2015, pp. 224–243.
doi:10.1016/j.actamat.2015.04.050
[40] Weetman, P., and Akhras, G., "Modeling a Galfenol Based Stress Sensor Capable of Sensing Up to Three Axial Stresses," *Journal of Applied Physics*, Vol. 114, No. 18, 2013, Paper 183911.
doi:10.1063/1.4831666

[41] Boesenberg, A., Restorff, J., Wun-Fogle, M., Sailsbury, H., and Summers, E., "Texture Development in Galfenol Wire," *Journal of Applied Physics*, Vol. 113, No. 17, 2013, Paper 17A909. doi:10.1063/1.4794186

[42] Domann, J., Loeffler, C., Martin, B., and Carman, G., "High Strain-Rate Magnetoelasticity in Galfenol," *Journal of Applied Physics*, Vol. 118, No. 12, 2015, Paper 123904. doi:10.1063/1.4930891

[43] Cao, H., Gehring, P. M., Devreugd, C., Rodriguez-Rivera, J., Li, J., and Viehland, D., "Role of Nanoscale Precipitates on the Enhanced Magnetostriction of Heat-Treated Galfenol (Fe 1- x Ga x) Alloys," *Physical Review Letters*, Vol. 102, No. 12, 2009, Paper 127201. doi:10.1103/PhysRevLett.102.127201

[44] Kellogg, R. A., "Development and Modeling of Iron-Gallium Alloys," Ph.D. Thesis, Iowa State Univ., Ames, IA, 2003.

[45] Clark, A., Wun-Fogle, M., Restorff, J., and Lograsso, T., "Magnetic and Magnetostrictive Properties of Galfenol Alloys Under Large Compressive Stresses," *Proceedings of Pacific Rim International Conference on Advanced Materials and Processing*, Vol. 11, Honolulu, HI, Dec. 2001.

[46] Summers, E. M., Lograsso, T. A., Snodgrass, J. D., and Slaughter, J. C., "Magnetic and Mechanical Properties of Polycrystalline Galfenol," *Smart Structures and Materials*, International Society for Optics and Photonics, Bellingham, WA, 2004, pp. 448–459, https://lib.dr.iastate.edu/ameslab_conf/59/. doi:10.1117/12.539781

[47] Clark, A. E., Restorff, J. B., Wun-Fogle, M., Lograsso, T. A., and Schlagel, D. L., "Magnetostrictive Properties of Body-Centered Cubic Fe–Ga and Fe–Ga–Al Alloys," *IEEE Transactions on Magnetics*, Vol. 36, No. 5, 2000, pp. 3238–3240. doi:10.1109/20.908752

[48] Clark, A. E., Wun-Fogle, M., Restorff, J. B., and Lograsso, T. A., "Magnetostrictive Properties of Galfenol Alloys Under Compressive Stress," *Materials Transactions*, Vol. 43, No. 5, 2002, pp. 881–886. doi:10.2320/matertrans.43.881

[49] Kellogg, R., Flatau, A. B., Clark, A., Wun-Fogle, M., and Lograsso, T. A., "Temperature and Stress Dependencies of the Magnetic and Magnetostrictive Properties of Fe 0.81 Ga 0.19," *Journal of Applied Physics*, Vol. 91, No. 10, 2002, pp. 7821–7823. doi:10.1063/1.1452216

[50] Ueno, T., Summers, E., and Higuchi, T., "Machining of Iron–Gallium Alloy for Microactuator," *Sensors and Actuators A: Physical*, Vol. 137, No. 1, 2007, pp. 134–140. doi:10.1016/j.sna.2007.02.026

[51] Liu, R., Agrawal, A., Liao, W.-K., Choudhary, A., and Chen, Z., "Pruned Search: A Machine Learning Based Meta-Heuristic Approach for Constrained Continuous Optimization," *2015 Eighth International Conference on Contemporary Computing (IC3)*, IEEE Publ., Piscataway, NJ, 2015, pp. 13–18. doi:10.1109/IC3.2015.7346645

[52] Lewis, R. M., and Torczon, V., "Pattern Search Algorithms for Bound Constrained Minimization," *SIAM Journal on Optimization*, Vol. 9, No. 4, 1999, pp. 1082–1099. doi:10.1137/S1052623496300507

[53] Lewis, R. M., and Torczon, V., "Pattern Search Methods for Linearly Constrained Minimization," *SIAM Journal on Optimization*, Vol. 10, No. 3, 2000, 917–941. doi:10.1137/S1052623497331373

[54] Audet, C., and Dennis, J. E. Jr, "Analysis of Generalized Pattern Searches," *SIAM Journal on Optimization*, Vol. 13, No. 3, 2002, pp. 889–903. doi:10.1137/S1052623400378742

[55] Audet, C., and Dennis, J. E. Jr, "A pattern Search Filter Method for Nonlinear Programming Without Derivatives," *SIAM Journal on Optimization*, Vol. 14, No. 4, 2004, pp. 980–1010. doi:10.1137/S105262340138983X

[56] Rigoni, E., and Turco, A., "Metamodels for Fast Multi-Objective Optimization: Trading Off Global Exploration and Local Exploitation," *Asia-Pacific Conference on Simulated Evolution and Learning*, Springer, New York, 2010, pp. 523–532. doi:10.1007/978-3-642-17298-4_56

[57] Gondzio, J., and Terlaky, T., "A Computational View of Interior Point Methods," *Advances in Linear and Integer Programming*, Oxford Univ. Press, Oxford, England, U.K., 1996, p. 103.

[58] Downey, P., and Flatau, A., "Magnetoelastic Bending of Galfenol for Sensor Applications," *Journal of Applied Physics*, Vol. 97, No. 10, 2005, Paper 10R505. doi:10.1063/1.1853838

[59] Datta, S., and Flatau, A. B., "Magnetostrictive Vibration Sensor Based on Iron-Gallium Alloy," *MRS Proceedings*, Vol. 888, Cambridge Univ. Press, New York, 2005, Paper 0888–V04-09. doi:10.1557/PROC-0888-V04-09

[60] Torczon, V., "On the Convergence of Pattern Search Algorithms," *SIAM Journal on Optimization*, Vol. 7, No. 1, 1997, pp. 1–25. doi:10.1137/S1052623493250780

R. Ohayon
Associate Editor